Simulation of a guitar amplifier stage for several triode models: examination of some relevant phenomena and choice of adapted numerical schemes

Ivan Cohen, Thomas Hélie

Audio Engineering Society

Convention Paper

Presented at the 127th Convention
2009 October 9–12 New York NY, USA

Simulation of a guitar amplifier stage for several triode models: examination of some relevant phenomena and choice of adapted numerical schemes

Ivan Cohen[1] [2], and Thomas Helie [1]

[1] *Ircam - CNRS - STMS UMR 9912, Analysis/Synthesis Team, Paris, France*

[2] *Orosys R&D, Montpellier, France*

Correspondence should be addressed to Ivan Cohen, Thomas Helie (ivan.cohen@orosys.fr, thomas.helie@ircam.fr)

ABSTRACT

This paper deals with the simulation of a high gain triode stage of a guitar amplifier. Triode models taking into account various "secondary phenomena" are considered and their relevance on the stage is analyzed. More precisely, both static and dynamic models (including parasitic capacitances) are compared. For each case, the stage can be modeled by a nonlinear differential algebraic system. For static triode models, standard explicit numerical schemes yield efficient stable simulations of the stage. However, the effect due to the capacitances in dynamic models is audible (Miller effect) and must be considered. The problem becomes stiff and requires the use of implicit schemes. The results are compared for all the models and corresponding VST plug-ins have been implemented.

1. INTRODUCTION

Many analog audio circuit simulations (guitar amplifiers, synthesizers, studio devices etc.) have been released for musicians, who want to replace their equipment with cheaper and more flexible digital equivalents (hardware or software). Nevertheless, the realism of these digital simulations can still be improved. This is mainly due to some nonlinearities that are responsible for the "sound signature of analog audio devices" the modeling of which is often

complex and still keeps a lot of people busy.

This paper deals with the simulation of guitar tube amplifiers for real-time applications. These devices are composed of three main parts : the preamplifier, power amplifier, and power supply. Moreover, their "sound signatures" follow from designers' choices (location of the tonestack, specific cutoff frequencies, polarization of tube stages etc.). In this article, the behavior of a typical 12AX7 triode stage of a high gain preamplifier is studied, for static and dynamic triode models, with well-suited numerical schemes and implementations of real-time numerical simulations.

2. THE COMMON CATHODE TRIODE AMPLIFIER

2.1. Presentation

The common cathode triode amplifier is a topology of circuit that has been used in hi-fi and guitar amplifiers to increase the voltage of a signal. It has interesting properties in terms of sound for musicians and audiophiles, which justifies its use today, several years after the apparition of transistors (for example the harmonic content of the triode saturation [1]), and its study in papers about guitar amplifiers simulation [5] [6] [7] [8] [9]. It is found in most of the guitar preamplifiers, which have the purpose to increase the voltage of the guitar's signal (with a maximum voltage of 400 mV, and an impedance of 20 kΩ, depending on the type of guitar pickup), and to enrich its tone. The triode chosen by designers is very often a 12AX7 (also called ECC83).

2.2. Electronic circuit

The electronic circuit can be seen in figure 1, with values for its components in the table 1.

Rp	Rg	Ro	Rk
100 KΩ	220 KΩ	22 KΩ	2.7 KΩ
Vbias	Co	Ck	
300 V	20 nF	10 μF	

Table 1: Typical values of components used in the common cathode triode amplifier

The triode is a current source controlled by a voltage, and can be considered as a voltage source if we connect the cathode to the ground, and the plate to a constant voltage source V_{bias} and a load resistance

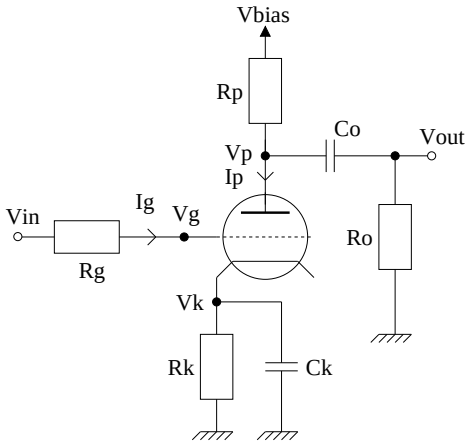

Fig. 1: The common cathode triode amplifier

R_p. To increase the performances of this topology, the resistance R_k is added between the cathode and the ground, to polarize the input voltage, with a decoupling condensator C_k in parallel, which limits the variation of the cathode bias potential. The resistance R_g limits the grid rectification effect (see next section for explanations). The R_o and C_o coupling components allow the designer to add several triode amplifiers in cascade, if more distortion of harmonics is needed in the output signal. The condensator suppresses the DC component of the signal, the resistance changes the output gain of the electronic stage, and they act together as a high-pass filter [2].

2.3. Electronic equations

For this study, the resistances and capacitors are considered ideal, and the triode as a set of two current sources (see figure 2), controlled by the voltages of its poles, the grid (g), the cathode (k) and the plate (p). The influence of the heater is neglected. The triode modeled is a generic 12AX7 / ECC83.

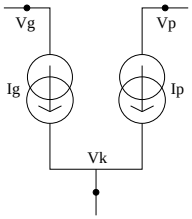

Fig. 2: The triode's model

Using the Millman's theorem, the electronic circuit

can be modeled by a set of differential algebraic equations :

$$\begin{aligned} \frac{V_g}{R_g} &= -I_g + \frac{V_{in}}{R_g} \\ \frac{V_p}{R_p} + C_o\frac{\mathrm{d}V_p}{\mathrm{d}t} &= -I_p + \frac{V_{bias}}{R_p} + C_o\frac{\mathrm{d}V_{out}}{\mathrm{d}t} \\ \frac{V_k}{R_k} + C_k\frac{\mathrm{d}V_k}{\mathrm{d}t} &= I_p + I_g \\ \frac{V_{out}}{R_o} + C_o\frac{\mathrm{d}V_{out}}{\mathrm{d}t} &= C_o\frac{\mathrm{d}V_p}{\mathrm{d}t} \end{aligned} \quad (1)$$

where I_p and I_g are functions set by a not trivial choice of the triode's model. In the next sections, the triode behavior and its modeling will be the object of a particular attention.

3. STATIC TRIODE MODELS

3.1. Introduction

The 12AX7 triode is a vacuum tube diode, with a negative grid to cathode voltage Vgk controling the electron flux, generated by the heater from the cathode to the plate. The currents I_p and I_g are always positive, up to a few mA. The 12AX7 is a high gain triode, with its gain parameter μ around 100. Datasheets - available on the internet - show graphs of the function $I_p = f(Vgk, Vpk)$, got from measures.

3.2. Triode models

For the first modeling, we focus on the static triode models of Leach [3] and Norman Koren [4], which are standard and broadly used. They model the triode as two current sources which are a function of the voltages V_{pk} and V_{gk} :

$$\begin{aligned} I_p &= L_p(V_{gk}, V_{pk}) \\ I_g &= L_g(V_{gk}, V_{pk}) \end{aligned} \quad (2)$$

where L_p and L_g are nonlinear functions.

3.2.1. Leach's model

The Leach's model is derived from the Child-Langmuire law [3] [5], and also gives an expression for the current I_g.

$$\begin{aligned} L_p &= \begin{cases} K(\mu V_{gk} + V_{pk})^{3/2} & \text{if } (\mu V_{gk} + V_{pk}) > 0 \\ 0 & \text{else} \end{cases} \\ L_g &= \begin{cases} 0 & \text{if } V_{gk} < V_\gamma \\ \frac{V_{gk} - V\gamma}{R_{gk}} & \text{else} \end{cases} \end{aligned} \quad (3)$$

The following table gives typical values for the model parameters, from [4] and SPICE models. The figures 4 and 3 show the dependance of I_p with V_{gk} and V_{pk}.

μ	K	Rgk	$V\gamma$
88.5	1.73×10^{-6}	20 kΩ	0.6 V

Table 2: Typical values for Leach's model parameters

3.2.2. Norman Koren's model

Derived from the Leach model, Norman Koren's model is "phenomenological", which models the behavior of physical phenomena using parameters not derived from fundamental physics. It has been designed so that plate current $I_p > 0$ whenever plate voltage $V_{pk} > 0$ [4]. It matches better published curves from datasheets. The expression of the L_p function is the following :

$$\begin{aligned} E_1 &= \frac{V_{pk}}{K_p}\ln\left[1 + \exp\left(K_p\left(\frac{1}{\mu} + \frac{V_{gk}}{\sqrt{K_{vb} + V_{pk}^2}}\right)\right)\right] \\ L_p &= \frac{E_1^{E_x}}{K_g}(1 + \mathrm{sgn}(E_1)) \end{aligned} \quad (4)$$

The following table gives typical values for the model parameters, from [4] and SPICE models. The figures 5 and 6 show the dependance of I_p with V_{gk} and V_{pk}.

μ	K_p	K_{vb}	K_g	Ex
88.5	600	300	1060	1.4

Table 3: Typical values for Norman Koren's model parameters

3.3. Grid rectification effect

The I_g current is often neglected in simulations, but it is responsible for the grid rectification effect that designers try to contain using specific polarization. When the grid-to-cathode voltage V_{gk} becomes positive, the value of I_g increases by a few mA. As a

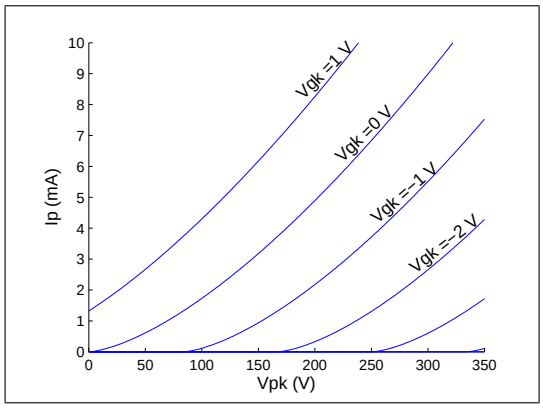

Fig. 3: I_p function of Vpk for the Leach's model

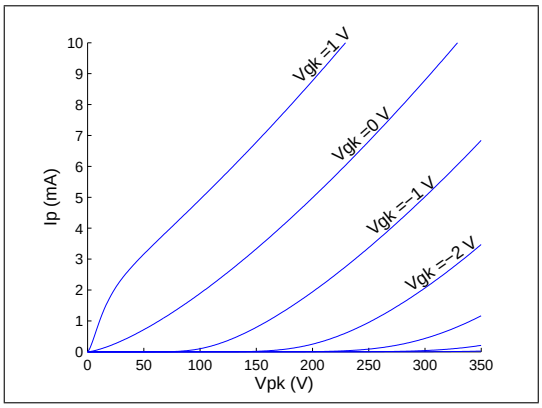

Fig. 5: I_p function of Vpk for the Koren's model

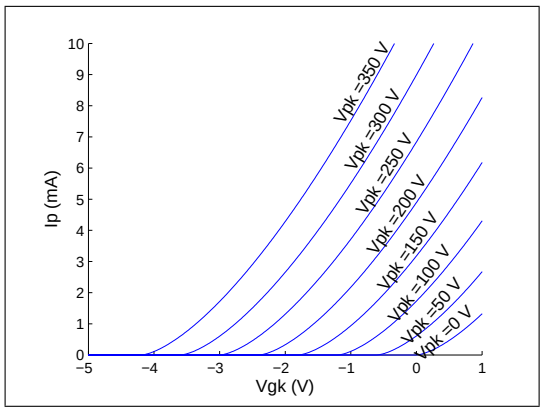

Fig. 4: I_p function of Vgk for the Leach's model

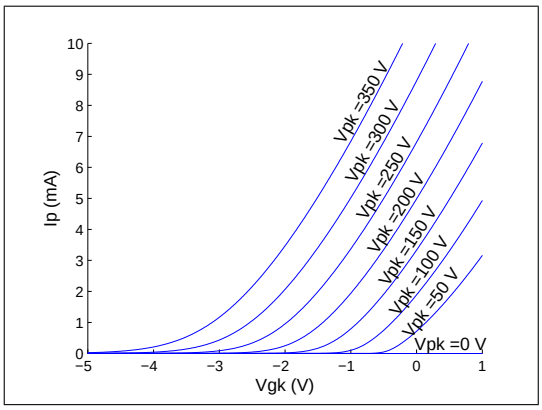

Fig. 6: I_p function of Vgk for the Koren's model

result, the voltage measured at the grid in the common cathode triode is limited in its positive course. The triode acts like a rectifier.

One of the uses of the resistance R_g is to control the amount of the grid rectification effect. This is why it is usually chosen with high values. Another use of this resistance will be seen in the study of the dynamic triode models.

This kind of distortion is not wanted by electronic designers, but exists, and is modeled to increase the realism of the simulation. More, it is one of the reasons of the plate voltage saturation.

Complex ways to model this current are described in SPICE circuits, like replacing the current source by a diode and a resistance, but the adopted model for the current I_g is the expression from the Leach's model in this work (see figure 7), as a first study of the grid rectification effect. Improvements will be done in a future work using measures.

Next, deriving the equations of the circuit for these models leads to nonlinear differential algebraic systems, with a state-space-like representation.

3.4. Extended state-space representations

3.4.1. Introduction

Linear state-space representations are well known in automatics. Let X be the dynamic state vector of the studied system, U the input vector and Y the output vector. A, B, C and D are the matrix which express the behavior of the linear system.

$$\begin{aligned} dX/dt &= AX + BU \\ Y &= CX + DU \end{aligned} \tag{5}$$

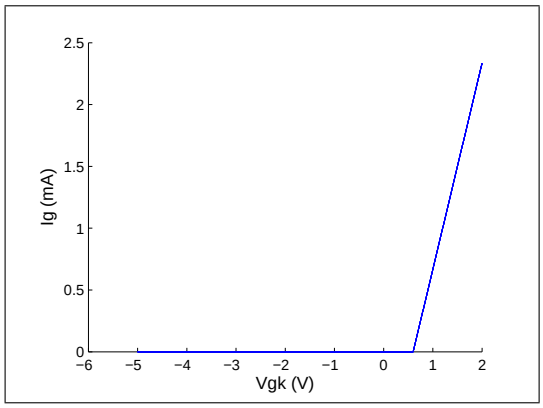

Fig. 7: I_g function of Vpk

For nonlinear cases, the expression of dX/dt and Y can be replaced with nonlinear functions of X and U. Moreover, the nonlinearity can introduce implicit equations. They are expressed using a static nonlinear state vector W, and added to the state space representation.

$$\begin{aligned} dX/dt &= f(X,W,U) \\ 0 &= g(X,W,U) \\ Y &= h(X,W,U) \end{aligned} \tag{6}$$

3.4.2. State-space equations of the triode amplifier

The dynamic behavior of the circuit is caused by the condensators. The nonlinearity comes from the triode modeling, and the expression of the currents I_p and I_g. Therefore, the condensators voltages have been chosen as the dynamic state variables, and the triode potentials as the static nonlinear state variables, which have an implicit expression. Let the state variables be :

$$\begin{aligned} U &= V_{in} \\ X &= [V_k \quad V_{out} - V_p]^T \\ W &= [V_p \quad V_g]^T \\ Y &= V_{out} \end{aligned} \tag{7}$$

The dimension of the vectors X and W are both equal to two. The state space representation of the triode stage is the following :

$$\begin{aligned} f(X,W,U) &= \begin{cases} -\frac{X_1}{R_k C_k} + \frac{I_g+I_p}{C_k} \\ -\frac{X_2+W_1}{R_o C_o} \end{cases} \\ g(X,W,U) &= \begin{cases} W_1 + R_p(I_p + \frac{X_2+W_1}{R_o}) - V_{bias} \\ W_2 - U + R_g I_g \end{cases} \\ h(X,W,U) &= X_2 + W_1 \end{aligned} \tag{8}$$

with

$$\begin{aligned} I_p &= L_p(W_2 - X_1, W_1 - X_1) \\ I_g &= L_g(W_2 - X_1, W_1 - X_1) \end{aligned} \tag{9}$$

This extended state space representation yields to a numerical simulation with standard methods of resolution, for differential and implicit equations.

3.5. Resolution of differential equations and numerical schemes

The notation Z_n indicates the state of the variable Z for the n-th sample. For each sample, X_n is determined using methods of resolution for the differential equations $dX/dt = f(X,W,U)$, and then the zeros of $0 = g(X,W,U)$ give W_n with implicit equations resolution methods.

3.5.1. Differential equations

Let T_e be the sampling period and F_e the sampling frequency. A method to resolve differential equations in the discrete domain is to approximate dX/dt with $F_e \times (X_{n+1} - X_n)$. This is the explicit Euler method (see equation 10).

$$X_{n+1} = X_n + T_e f(X_n, W_n, U_n) \tag{10}$$

In general, we prefer to use explicit Runge-Kutta methods instead of explicit Euler, for stability and accuracy considerations [10]. The resolution of the function $dX/dt = f(X,W,U)$ will be done with the Runge-Kutta second order method (see equation 12).

$$\begin{aligned} k_1 &= T_e f(X_n, W_n, U_n) \\ X_{n+1} &= X_n + T_e f(X_n + \frac{k_1}{2}, W_n, \frac{U_n + U_{n+1}}{2}) \end{aligned} \tag{11}$$

3.5.2. Implicit equations

The equation $0 = g(X,W,U)$ is implicit. The standard method of Newton-Raphson is used to find the

value of W, which satisfies the implicit equation $0 = g(X, W, U)$, for constant values of X and U. This algorithm is iterative, and converges to a solution for W.

Let W_n^k be the approximated value of W at the iteration k of the algorithm for the sample n. $J(g(X, W, U))$ is the Jacobian matrix of $g(X, W, U)$, derived with respect to the vector W.

$$W_n^{k+1} = W_n^k - J^{-1}(g(X_n, W_n^k, U_n)) \times g(X_n, W_n^k, U_n) \quad (12)$$

If W_n^0 is close to the solution, the algorithm converges faster. Because the variation of W between two samples can be considered low if the sampling frequency F_e is high, W_{n-1} is chosen as the initialization value.

The number of iterations done for each sample is constant. Studying the error on W and the speed of its convergence reveals that four iterations for the Newton-Raphson algorithm are sufficient. This numerical scheme is efficient and stable, and has been implemented in a real-time application as a VST plug-in for the two triode models.

3.6. Comparisons

The simulations with the static triode models of Leach and Norman Koren are compared. First, the curves of the function L_p are compared to the ones found in the datasheets of the 12AX7. It appears that the Norman Koren's model is more realistic than the Leach's one, it models the behavior of the triode better for high grid and plate voltages.

Second, the behavior of the simulated circuit is observed. A sine waveform with a frequency of 200 Hz and an amplitude of 10 V is used to feed the input of the triode stage. The consideration of the I_g current is essential in the two cases, and changes the maximum of the grid voltage, which can feed the triode according to the rectification effect. Without taking it into account, the grid voltage can be very high, exceeding the physical limit of voltage the real triode's grid can handle, and command impossible voltages like a negative V_p voltage with the Leach's model.

As a result, Norman Koren's static triode model is chosen as the most efficient.

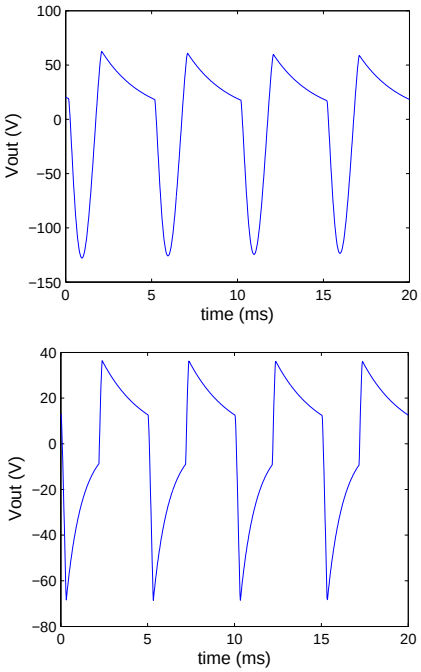

Fig. 8: Output signal for Leach's model (respectively without and with the I_g current)

4. DYNAMIC TRIODE MODELS

The accuracy of the triode model can be increased if its dynamic behavior is considered. It is modeled from the Norman Koren's static model, including three parasitic capacitances between its poles.

4.1. Parasitic capacitances and Miller effect

The capacitance values of table 4 are taken from the datasheets, for C_{gp} (grid-plate), C_{gk} (grid-cathode) and C_{pk} (plate-cathode).

Cgp	Cgk	Cpk
1.7 pF	1.8 pF	1.9 pF

Table 4: Typical values for parasitic capacitances of the 12AX7

Although the capacitances are low, they significantly change the frequency response of the triode stage, due to the Miller effect [11]. The linearization of the equations of the new circuit, around an equilibrium point for a constant input voltage $U*$, demonstrates the capacitance C_{gp} is multiplied by a gain, contrary

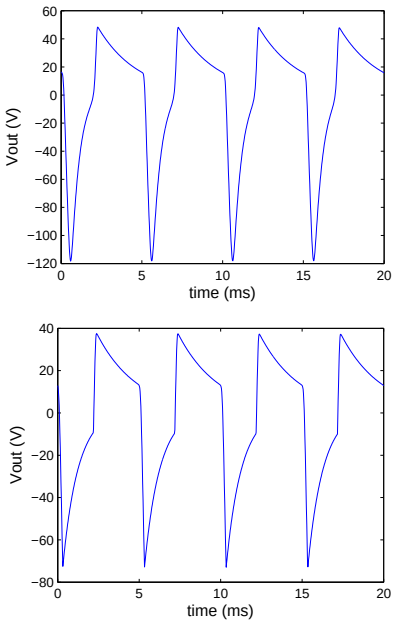

Fig. 9: Output signal for Koren's model (respectively without and with the I_g current)

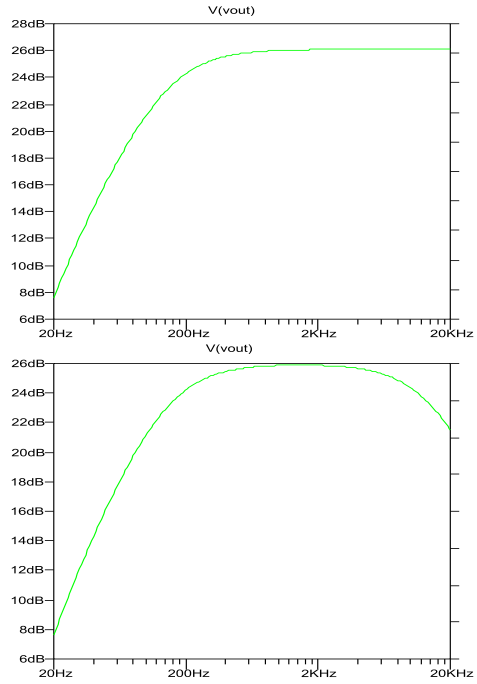

Fig. 10: Frequency response

to the two other capacitances, and acts in combination with R_g as a lowpass filter, with a minimum cutoff frequency at 5 kHz. These results have been confirmed using SPICE [12] simulations and are audible. The other capacitances have a very low influence on the frequency response, and have therefore been neglected in the following study. The difference between the frequency response of the triode stage with and without the parasitic capacitances are shown in the figure 10.

4.2. New circuit and new equations

The circuit seen in figure 11 is the same triode amplifier as before, taking the parasitic capacitance Cgp of the 12AX7 into account, and yields to a new set of equations, resulting from the Millman's theorem.

$$\begin{aligned}
\frac{V_k}{R_k} + C_k\frac{\mathrm{d}V_k}{\mathrm{d}t} &= I_g + I_p \\
\frac{V_g}{R_g} + C_{gp}\frac{\mathrm{d}V_g}{\mathrm{d}t} &= -I_g + \frac{V_{in}}{R_g} + C_{gp}\frac{\mathrm{d}V_p}{\mathrm{d}t} \\
\frac{V_p}{R_p} + (C_o + C_{gp})\frac{\mathrm{d}V_p}{\mathrm{d}t} &= -I_p + \frac{V_{bias}}{R_p} \\
&\quad + C_o\frac{\mathrm{d}V_{out}}{\mathrm{d}t} + C_{gp}\frac{\mathrm{d}V_g}{\mathrm{d}t} \\
\frac{V_{out}}{R_o} + C_o\frac{\mathrm{d}V_{out}}{\mathrm{d}t} &= C_o\frac{\mathrm{d}V_p}{\mathrm{d}t} \qquad (13)
\end{aligned}$$

Adding a capacitance in the circuit does not add an equation in the system. As a result, the dimension of the vector X becomes three, and the new dimension of W is one. The new state-space variables are :

$$\begin{aligned}
U &= V_{in} \\
X &= [V_k \quad V_{out} - V_p \quad V_g - V_p]^T \\
W &= V_p \\
Y &= V_{out} \qquad (14)
\end{aligned}$$

The extended state-space representation of the sys-

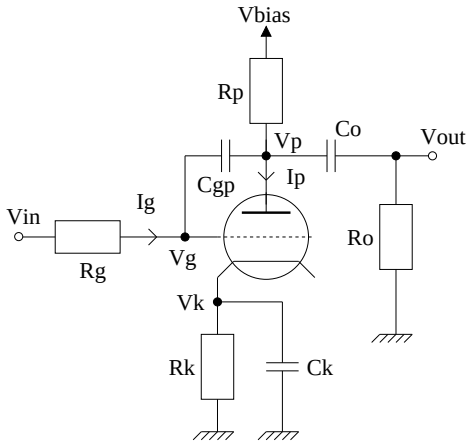

Fig. 11: The common cathode triode amplifier with the parasitic capacitance Cgp

tem becomes the following.

$$\begin{aligned} f(X,W,U) &= \begin{cases} -\frac{1}{R_k C_k} X_1 + \frac{1}{C_k}(I_g + I_p) \\ -\frac{1}{R_o C_o}(X_2 + W_1) \\ \frac{1}{C_{gp}}(-I_g + \frac{U - X_3 - W_1}{R_g}) \end{cases} \\ g(X,W,U) &= \frac{W_1 - V_{bias}}{R_p} + I_p + I_g + ... \\ & \quad \frac{-U}{R_g} + \frac{X_2 + W_1}{R_o} + \frac{X_3 + W_1}{R_g} \\ h(X,W,U) &= X_2 + W_1 \end{aligned} \tag{15}$$

with

$$\begin{aligned} I_p &= L_p(X_3 + W_1 - X_1, W_1 - X_1) \\ I_g &= L_g(X_3 + W_1 - X_1, W_1 - X_1) \end{aligned} \tag{16}$$

4.3. Stiff problems and stability

The simulation of the new set of equations, using the previous numerical scheme, is not stable. Indeed, the parasitic capacitance C_{gp}, with its very low value, can involve high derivatives of the vector X : a stiff problem appears.

There is no rigorous definition of stiffness in the literature, but it can be considered as a differential equation for which certain numerical methods for solving the equation are numerically unstable, with some terms that can lead to rapid variation in the solution. This requires the use of implicit numerical schemes, like implicit Euler methods (see equation 17). The Newton-Raphson algorithm is used for both the resolution of the dynamic and nonlinear implicit equations.

$$X_{n+1} = X_n + T_e f(X_{n+1}, W_{n+1}, U_{n+1}) \tag{17}$$

This new numerical scheme is stable and implemented as a VST plug-in too.

4.4. Comparisons

The new triode model takes more parameters into account than the static ones. The parasitic capacitance changes the frequency response of the triode stage, and the results are audible. With the same sinusoid than before as an input, we can see that the output signal waveform has a different shape and a different harmonic content, which matches with the equivalent simulation results in SPICE [12], considered as our reference for the numerical schemes. Changing a linear element inside a dynamic and nonlinear system with delay free loops changes the way the signal is distorted and in a complex way that cannot be modeled by a simple additional filter inside the signal chain.

Alternatively, the need for Newton-Raphson algorithm's for both differential equations and nonlinear implicit equations has a cost, in terms of CPU consumption, which is not negligible for real-time applications. Code optimization will become necessary for the simulation of more stages and full guitar amplifiers, using for example tables and interpolation algorithms.

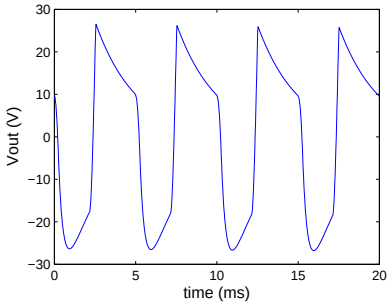

Fig. 12: Output signal for the dynamic triode's model

5. DISCUSSION

The choice of the sampling frequency (96 kHz in our case) is very important, for three reasons. First,

the use of high sampling frequencies or oversampling functions is recommended for nonlinear digital simulations, to avoid the apparition of aliasing in the audible frequencies. Secondly, the differential equations resolution algorithms use F_e as a step, so increasing the sampling frequency increases the accuracy of the processing. Lastly, the more the sampling frequency is important, the less is the variation of W between two samples. The convergence of the Newton-Raphson algorithm is faster if its initial value is close to the solution W of the equation $g(X, W, U) = 0$. As such, increasing the sampling frequency increases the convergence's speed of Newton-Raphson's algorithm for a given number of iterations.

In realistic terms, the simulation of the triode stage is able to produce signals with a rich harmonic content, if the gain of the input signal is high enough. Three or four triode stages in cascade, with a good cabinet simulation, result in a good approximation of a high gain guitar amplifier sound. Sound examples are available at `http://www.orosys.fr/cohen/aes127.htm`.

6. CONCLUSION

A preamplifier stage has been studied and simulated for Leach and Norman Koren's static models as well as dynamic versions, with efficient numerical schemes for real time applications. As a result, the Norman Koren's model combined with the parasitic capacitance C_{gp} was selected, for both objective and perceptive considerations. It yields to the implementation of plug-ins, which produces satisfactory sounds with standard cabinet simulations. Moreover, future work will be dedicated to model and simulate the other stages of a guitar amplifier, and to increase the efficiency of the electronic components models using measures.

7. REFERENCES

[1] Eric Barbour, "The Cool Sound of Tubes", IEEE Spectrum 35(8):24-35, 1998.

[2] Morgan Jones, "Valve Amplifiers, third edition", editions Newnes, 2003.

[3] W. Marshall Leach JR., "Spice models for vacuum tube amplifiers", in J. Audio Eng. Society, Vol. 43, No. 3, March 1995, pp. 117-126.

[4] Norman Koren, "Improved vacuum tube models for spice simulations", `http://www.normankoren.com`, 2003.

[5] Thomas Serafini, "A complete model of a tube amplifer stage", `http://www.simulanalog.org`, 2002.

[6] David T. Yeh and Julius O. Smith, "Simulating guitar distortion circuits, using wave digital and nonlinear state-space formulations", in Proc. of the 11th Int. Conf. on Digital Audio Effects (DAFx-08), Espoo, Finland, Sept. 1-4, 2008.

[7] Stefano Tubaro, Francesco Santagata, Augusto Sarti, "Non-linear digital implementation of a parametric analog tube ground cathode amplifier", in Proc. of the Int. Conf. on Digital Audio Effects (DAFx-07), Bordeaux, France, Sept. 10-15, 2007, pp. 169-172, `http://dafx.labri.fr/main/papers/p169.pdf`.

[8] Jyri Pakarinen, Matti Karjalainen, "Wave digital simulation of a vacuum-tube amplifier", in IEEE International Conference on Acoustics, Speech and Signal Processing (ICASSP06), May 2006.

[9] David T. Yeh, Jyri Pakarinen, "A review of digital techniques for modeling vacuum-tube guitar amplifiers", in Computer Music Journal Summer 2009, Vol. 33, No. 2, 2009.

[10] Jean-Pierre Demailly, "Analyse numerique et equations differentielles", Collection Grenoble Sciences, 2006.

[11] John M. Miller, "Dependence of the input impedance of a three-electrode vacuum tube upon the load in the plate circuit", in Scientific Papers of the Bureau of Standards, vol.15, no. 351, 1920.

[12] Linear Technology, "LTSpice IV / SwitcherCAD III", `http://www.linear.com`, 2009